

UNCLASSIFIED

AD 408 424

DEFENSE DOCUMENTATION CENTER
FOR
SCIENTIFIC AND TECHNICAL INFORMATION

CAMERON STATION, ALEXANDRIA, VIRGINIA



UNCLASSIFIED

NOTICE: When government or other drawings, specifications or other data are used for any purpose other than in connection with a definitely related government procurement operation, the U. S. Government thereby incurs no responsibility, nor any obligation whatsoever; and the fact that the Government may have formulated, furnished, or in any way supplied the said drawings, specifications, or other data is not to be regarded by implication or otherwise as in any manner licensing the holder or any other person or corporation, or conveying any rights or permission to manufacture, use or sell any patented invention that may in any way be related thereto.

63-4-2

CATALOGED BY DDC
AS AD No 408424

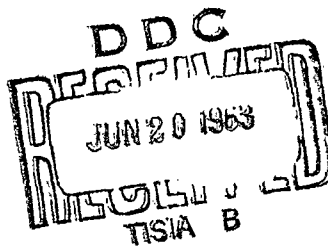
FINAL REPORT
Contract No. FAA/BRD-385

IMPROVED RADIO DOPPLER DETECTORS

March 1963

Project 426-1

REPORT NO. 1372-1



This report has been approved for general distribution.

408424

Prepared for

FEDERAL AVIATION AGENCY
SYSTEMS RESEARCH AND DEVELOPMENT SERVICE

by

AIRBORNE INSTRUMENTS LABORATORY
A DIVISION OF CUTLER-HAMMER, INC.
Deer Park, Long Island, New York

FINAL REPORT

Contract No. FAA/BRD-385

IMPROVED RADIO DOPPLER DETECTORS

by

John L. O'Connor and James B. Leary

March 1963

Project 426-1

REPORT NO. 1372-1

Prepared for

FEDERAL AVIATION AGENCY
SYSTEMS RESEARCH AND DEVELOPMENT SERVICE

by

AIRBORNE INSTRUMENTS LABORATORY
A DIVISION OF CUTLER-HAMMER, INC.
Deer Park, Long Island, New York

TABLE OF CONTENTS

	<u>Page</u>
Abstract	iii
I. Introduction	1
II. Conclusions	3
III. FM-CW X-Band Detectors	5
A. Theory of Operation	5
B. Basis of Technique	8
C. Circuit Description	15
D. Operating Procedures	26
IV. Dual-Antenna S-Band Detectors	31
V. Audio Analysis Equipment	36

LIST OF ILLUSTRATIONS

<u>Figure</u>		<u>Page</u>
1	Block Diagram of FM-CW Detector	6
2	Frequency-Time Plots	7
3	Frequency-Amplitude Plots	9
4	FM-CW Range Response	13
5	FM-CW X-Band Detector	16
6	Schematic Diagram of FM-CW Detector	17
7	Interconnection Diagram of FM-CW Detector	19
8	Simplified Schematic Diagram of Oscillator Multiplier (300 Unit)	21
9	Simplified Schematic Diagram of IF Amplifier and Second Mixer (200 Unit)	22
10	Simplified Schematic Diagram of Audio Amplifier (300 Unit)	24
11	Block Diagram of Power Supply (100 Unit)	25
12	Line Spectrum Resulting from Modulation Index of 3.2	29
13	Dual-Antenna S-Band Runway Detector	32
14	Block Diagram of Dual-Antenna S-Band Detector	33
15	Schematic Diagram of Approach-Zone Dual-Antenna S-Band Detector	35
16	Audio Analysis Equipment	37
17	Block Diagram of Audio Analysis Equipment	38
18	Schematic Diagram of Audio Analysis Equipment	39

ABSTRACT

This report describes the program of RF doppler detector improvement sponsored by the FAA and undertaken to eliminate deficiencies in the radio detectors used in the TRACE installation at NAFEC. Previous detectors detected aircraft but were also triggered by small, close-in, unwanted targets such as birds and rainfall.

Four X-band FM-CW doppler detectors and two dual-antenna CW S-band doppler detectors that were modified from GFE supplied by the FAA were developed under this program and delivered to NAFEC for test and experimentation. These detectors eliminate or greatly reduce detection of the unwanted targets by producing a "dead zone" immediately in front of the detector. The X-band FM-CW detector produces this zone where detection is eliminated by a frequency modulation technique, while the CW S-band unit uses physical separation of the receiver and transmitter antennas to achieve the same result. In addition, audio analysis equipment for storing and processing received signals was furnished to the FAA to aid in testing the equipment.

I. INTRODUCTION

In 1960, Airborne Instruments Laboratory (AIL) delivered to the Federal Aviation Agency (FAA) 22 S-band (2455 Mc) CW doppler detectors. These detectors were evaluated as part of the TRACE (Taxiing and Routing of Aircraft, Coordination Equipment) program by the FAA at the National Aviation Facilities Experimental Center (NAFEC).

During this evaluation, it was found that the sensors reliably detected aircraft passage but were susceptible to false excitation by birds and heavy rainfall.

To eliminate this shortcoming, AIL proposed to undertake a program to improve the detectors. The FAA awarded AIL Contract FAA/BRD-385, under which this report is written.

Two different techniques were evaluated and hardware that eliminated or greatly reduced unwanted detections was developed.

In the first approach, two of the original S-band CW detectors were fitted with separate transmitter and receiver antennas, which have lateral displacement. Insects, birds, or raindrops, though close enough to provide threshold target value, are not illuminated by both antennas.

In the second approach, four X-band detectors were developed, using a principle already used in doppler navigators to eliminate radome disturbance. By frequency-modulating the transmitter and tuning the receiver to a high-order (fifth) sideband in the transmitted spectrum, signal return varies directly with range within a preselected distance. This results in a deep null close to the detector

and renders the detector insensitive to unwanted excitation by close birds and rainfall.

Audio analysis equipment, capable of recording and analyzing target return, was also developed. A bank of octave-wide filters enables the operator to separate signal return into six bands of component frequencies as an aid in categorizing characteristics of wanted and unwanted signals.

II. CONCLUSIONS

The FM-CW doppler technique, on the basis of limited field tests, eliminates false detections within the predetermined dead zone. At the same time, it remains sensitive to targets within the detection zone. The dead zone extends radially from zero to 40 feet; the detection zone extends from 40 to 400 feet. These ranges vary somewhat according to target cross section, but can be considered typical. It should be emphasized that these zones were chosen as being most suitable for average conditions. In order to meet unusual operating requirements, simple electrical design changes can alter the frequency of the oscillator-multiplier and IF sections of the detector. These frequencies determine the range response of the detector. By proper selection almost any desired detection coverage can be obtained.

As shown by tests, the performance of the dual-antenna CW units is greatly improved during rainfall and presents an effective null against close-in targets. This null, caused by antenna displacement, is relatively short so that large birds at ranges of 10 to 20 feet may still cause an occasional false detection.

As previously stated, field tests on both equipments were limited; however, the results showed that the performance improved enough to warrant extensive evaluation tests at NAFEC. To measure the amount of improvement, it is recommended that the new and modified detectors be tested alongside the earlier version already installed at NAFEC.

Characteristic doppler returns from aircraft--that is, starting at a high frequency, reducing to zero, and returning to a high frequency--are unchanged by the new detector

techniques. However, the resultant audio frequency is four times as high for a given radial velocity in the X-band unit as in the S-band unit. The delivered audio analysis equipment contains recording and filtering facilities capable of processing either return. This equipment can be used in the evaluation tests to determine the feasibility of using the sequential output from adjacent frequency filters to establish target validity.

III. FM-CW X-BAND DETECTORS

A. THEORY OF OPERATION

The insensitivity of the FM-CW X-band detector to targets outside of a defined detection zone is produced by a modulation technique similar to that used in doppler navigators to eliminate radome disturbance.

Figure 1 contains a block diagram of the RF section of the FM-CW detector. RF energy is generated by the klystron, frequency-modulated by the oscillator, and passed to the directional coupler. The directional coupler delivers the RF energy to the antenna and delivers a small amount of power (20 db down) to the crystal mixer as local oscillator excitation.

Reflected energy from a target enters the antenna and goes through the directional coupler, as signal power, to the crystal mixer. The local-oscillator energy and the reflected signal energy heterodyne in the mixer and produce an IF signal.

The frequency-time plots show the operation of the RF section for targets at two ranges (Figure 2). Figure 2A shows that, for a target at zero range, the transmitted and reflected waves coincide. Figure 2B shows that, when the transmitted and reflected waves coincide, the difference frequency at the IF output of the crystal mixer is zero or DC. Figure 2C shows a time delay in the transmitted and reflected waves that occurs when the target is at some finite range. Figure 2D shows that a difference frequency exists for this condition.

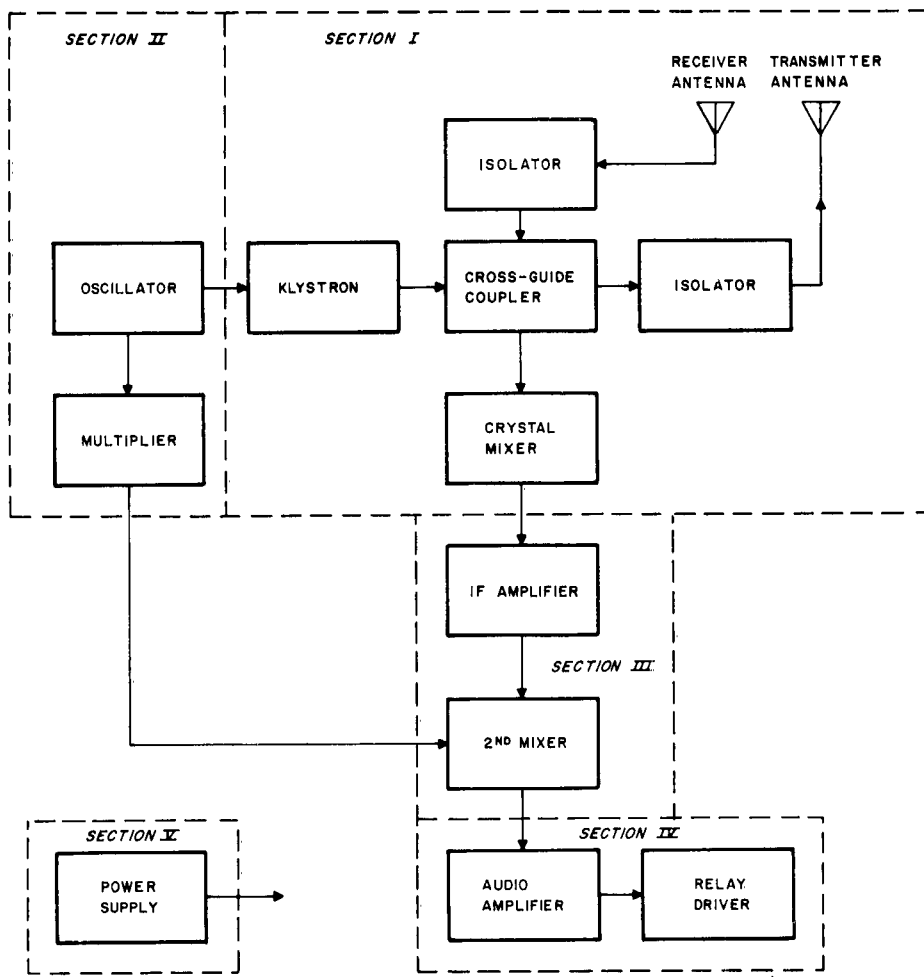


FIGURE 1. BLOCK DIAGRAM OF FM-CW DETECTOR

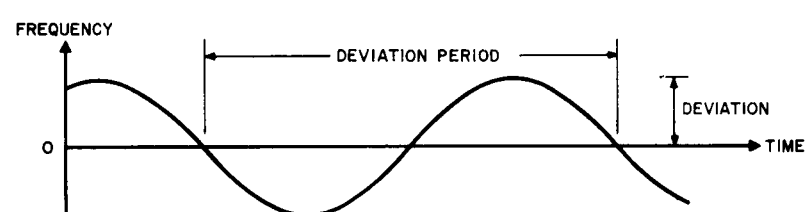
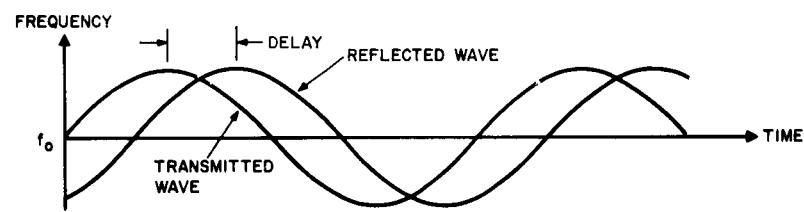
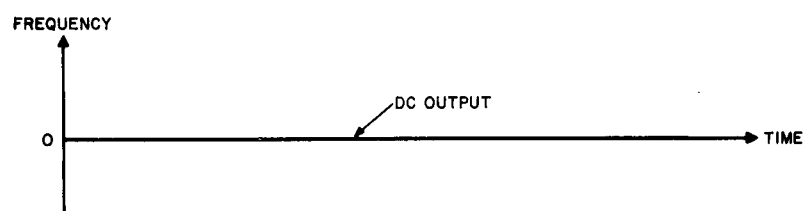
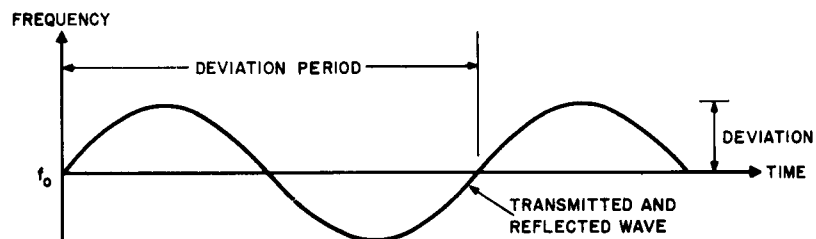


FIGURE 2. FREQUENCY-TIME PLOTS

Several things should be noted from the plots of Figure 2. A target will cause the effects shown in A and B not only if it is at zero range, but also if it is at a range that causes a transmission delay equal to a multiple of the deviation rate.

When a transmission delay exists (as shown in C), the difference frequency (shown in D) has the same deviation period as the transmitted wave. However, the deviation of the difference frequency depends upon the transmission delay and varies from zero deviation at zero delay to twice the deviation of the transmitted wave (when the delay is half the deviation-rate period).

The frequency-amplitude plots (Figure 3) are another representation of the difference frequency that exists at the IF output of the crystal mixer. The spectrum consists of individual lines spaced at the deviation rate. The amplitude of the spectrum lines depends upon the Bessel function of the modulation index (the deviation divided by the deviation rate). Figures 3A and 3B show that, although theoretically the spectrum exists at both positive and negative frequencies, it folds around zero frequency and produces sidebands of twice the theoretical amplitude.

Figure 3C shows that, since the deviation of the IF spectrum varies with the transmission delay, the amplitude of an individual sideband also varies with delay since it depends upon the Bessel function of the ratio of deviation to deviation rate. In addition, this variation is cyclic and repeats every deviation-rate period.

B. BASIS OF TECHNIQUE

The fact that the amplitude of each IF sideband is a function of the range of a target forms the basis of the discrimination by the FM-CW detector against nearby targets.

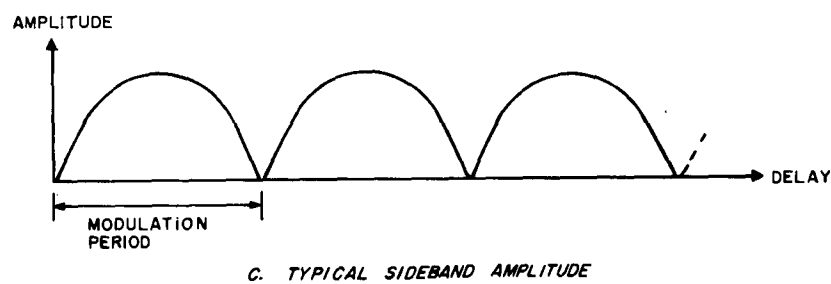
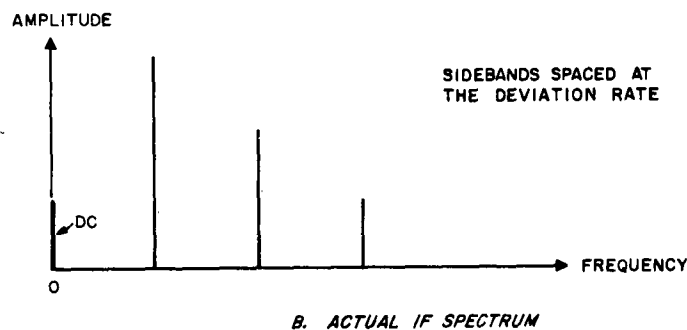
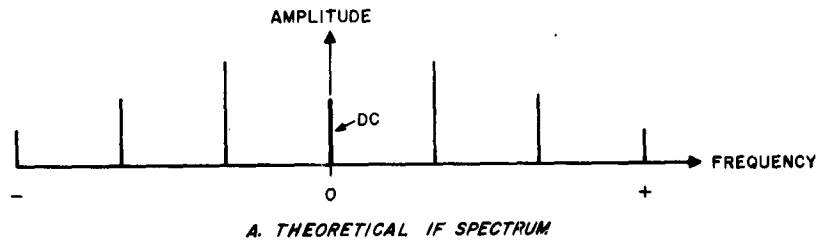


FIGURE 3. FREQUENCY-AMPLITUDE PLOTS

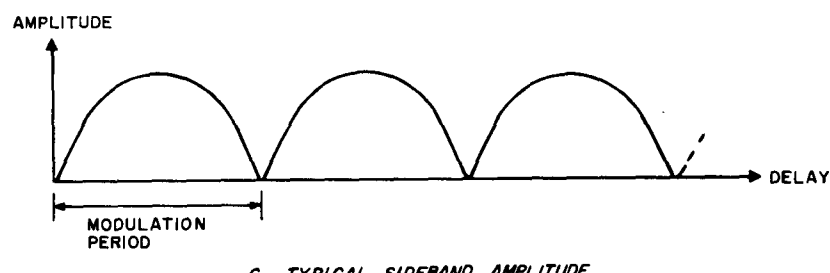
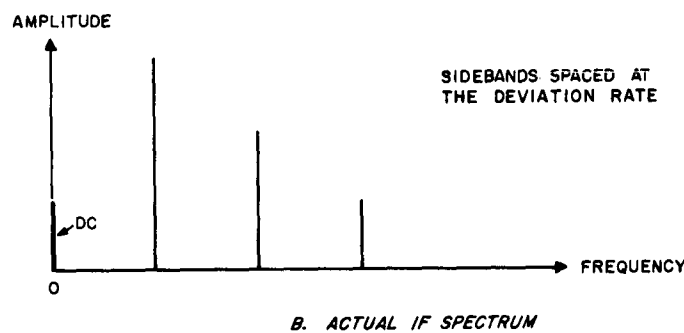
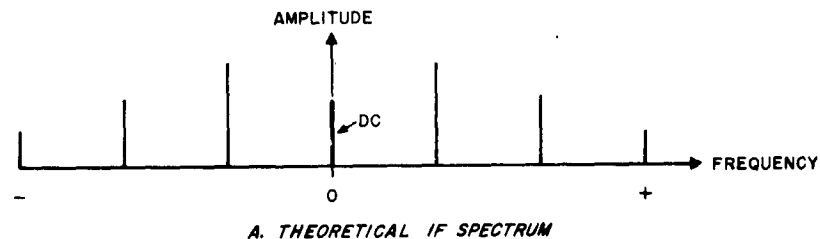


FIGURE 3. FREQUENCY-AMPLITUDE PLOTS

This section will analyze mathematically the operation of the RF section of the detector, choose some typical parameters, and then plot the expected range response of a detector having the chosen parameters.

An FM wave can be expressed by:

$$e_t = E_T \sin (\omega_c t + m \sin \omega_m t)$$

where

E_T = peak transmitted energy,
 ω_c = angular carrier frequency,
 ω_m = angular modulation frequency,
 m = modulation index given by ratio of peak frequency deviation to angular modulation frequency.

A return signal reflected from a target will be attenuated by some factor and will have a time delay. The received signal can be expressed by:

$$e_r = a E_T \sin \left[\omega_c (t + T) + m \sin \omega_m (t + T) \right]$$

where

T = transmission delay to and from target,
 a = losses encountered in travel to and from target.

Mixing is the product of transmitter leakage (factor b) and the received signal, and produces the following expression after mathematical manipulation:

$$b e_t e_r = \frac{ab E_T^2}{2} \cos \left[\omega_c T + 2 m \sin \frac{\omega_m T}{2} \cos \left(\omega_m t + \frac{\omega_m T}{2} \right) \right]$$

This can be recognized as an FM wave centered at DC ($\omega_c T$ = constant angular carrier frequency) with a modulation index of $2 m \sin \left(\frac{\omega_m T}{2} \right)$. In terms of the FM spectrum,

this means that the modulation index and, therefore, the energy in each sideband varies with the range of a target. This variation is cyclic and occurs at the modulation oscillator frequency.

Although this analysis has omitted many of the practical considerations, it is sufficient to explain the fundamental principle. It should be noted that this explanation has neglected the doppler shift upon which (as explained in later sections) the operation of the detector depends. Each spectrum line experiences a doppler shift if a moving target has produced the reflected signal. The detector recognizes the doppler shift as the result of a moving target and indicates a detection. It should also be noted that, because of the doppler shift, the phase difference between a pair of folded upper and lower sidebands occasionally reaches an odd multiple of 180 degrees, and the pair of side bands cancels itself. This gives rise to minor periodic nulls within the detection zone. Although the existence of these nulls at constant radii should be recognized, these nulls are not considered to be significant, because they are short in relation to target size and should be traversed rapidly by a passing target.

where

c = velocity of propagation in fps,
 f_m = modulating frequency,
 λ_m = modulating wavelength,
 R = desired maximum range to target in feet.

Therefore,

$$f = \frac{c}{2R}$$

To use the theory previously explained, useful values have to be assigned to the various parameters. The oscillator frequency is chosen to produce the desired coverage zone within the first sideband null.

$$\frac{c}{f_m} = \lambda_m = 2R$$

For example, for a range of 475 feet,

$$f = \frac{984}{2 \times 475} = 1.04 \text{ Mc}$$

The required power is determined from the various gains and losses in the system and can be divided into range attenuation and technique attenuation.

From the standard radar range equation, the power received as a reflection from a target is:

$$P_r = P_t \frac{G^2 \lambda^2 \sigma}{(4\pi)^3 R^4}$$

where

P_r = received power,

P_t = transmitted power,

G = detector antenna gain,

λ = wavelength of transmitting frequency,

R = range to target,

σ = target cross section.

Substituting typical values,

$$\frac{\lambda^2}{(4\pi)^3} = 4.4 \times 10^{-6} \quad (f = 10.525 \text{ Gc}),$$

where

$G = 10$ (for 70 x 20 degree antenna)

$\sigma = 100$ square feet (for a small aircraft target),

R = variable.

Figure 4 shows this expression plotted in decibels and labeled radar response.

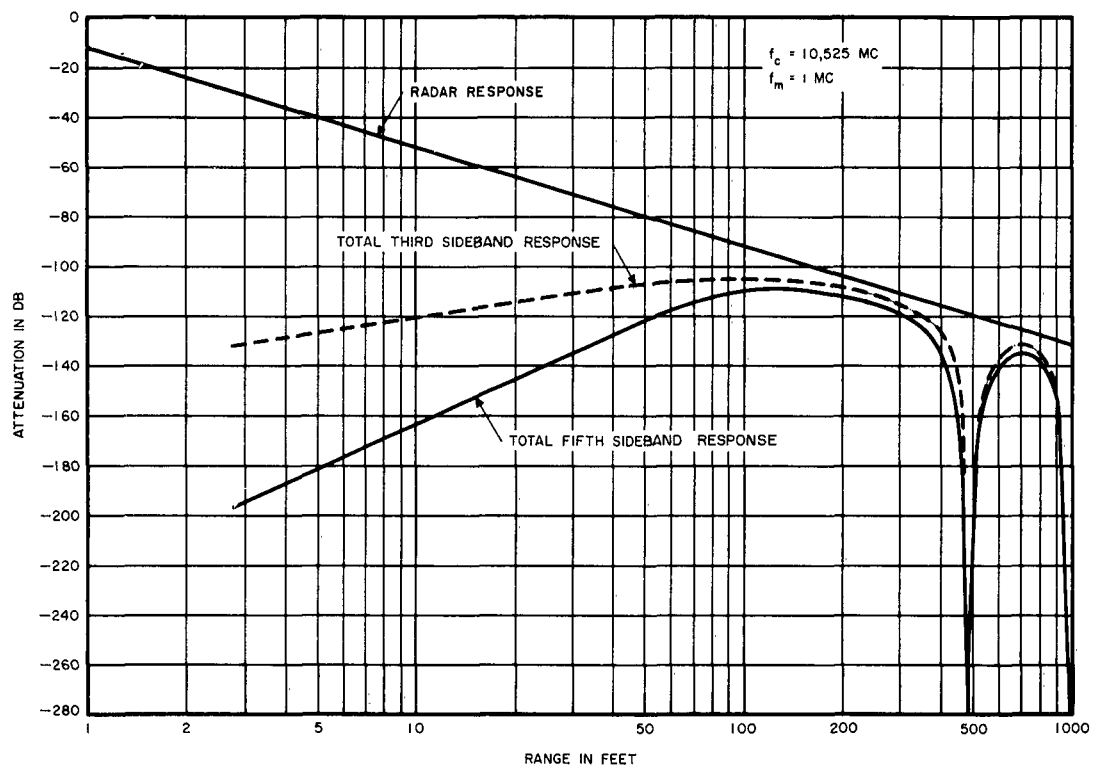


FIGURE 4. FM-CW RANGE RESPONSE

In addition to the radar response, the signal received by the detector experiences an attenuation because of the range-varying modulation index, which determines the energy in each sideband. This attenuation is referred to as the fm "technique attenuation."

The power in each sideband is given by:

$$J_n^2 \left[2m \sin\left(\frac{\omega_m T}{2}\right) \right] P_r$$

where

J_n = Bessel function of first order n ,

$n = 1, 2, 3, \dots$

m = modulation index,

ω_m = angular modulation frequency (1 Mc as selected),

T = transmission delay to target.

The modulation index is chosen for the sideband that is going to be used. The frequency deviation of a detector is adjusted so that the energy in the IF spectrum line of the chosen sideband will be a maximum.

Figure 4 combines the technique attenuation expression with the radar response curve to show the detector response for the third and fifth sidebands.

From the curve, it seems reasonable to use the fifth sideband to produce a good null in front of the detector. If a threshold is set at -136 db, the detector would have a response range from about 30 to 400 feet.

If a transmitted power of 40 mw or 16 dbm is assumed, a receiver sensitivity of -120 dbm is required. This can be realized for a narrow-band receiver of 2 kc and a noise figure of 20 db or better.

The following section, which contains the circuit description, also explains the manner in which the detector

recognizes the doppler shift of a target return and indicates a detection.

C. CIRCUIT DESCRIPTION

The FM-CW detector that has been developed is shown in Figure 5A as used in runway service but with cover removed. Figure 5B shows the unit adjusted for approach zone use with antennas pointed up. Complete circuit details with operating voltages are shown in schematic form in Figure 6 and unit interconnections are found in Figure 7.

1. RF SECTION

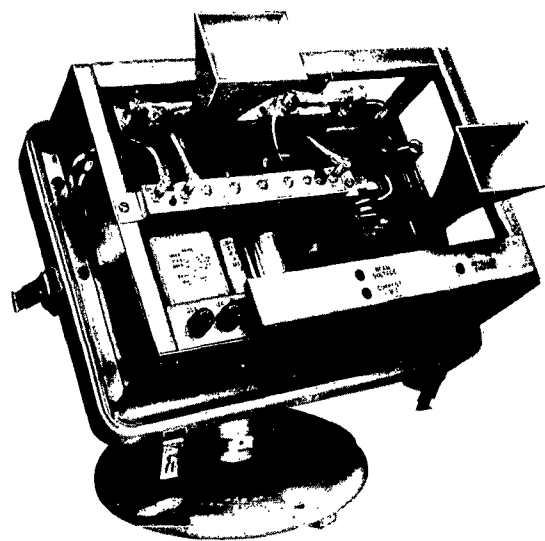
The RF section consists of two horn antennas whose beamwidths are 70 degrees (across the direction of aircraft passage) by 20 degrees (in line with the direction of aircraft travel) or 30 degrees (across) by 25 degrees (in line with), depending on whether the unit is intended for approach-zone or runway use (Section I of Figure 1).

A Varian VA-218B klystron is used as the transmitter tube. An isolator in the transmission path protects the klystron from any strong reflections that would cause impedance changes that could "pull" its operating frequency. The isolator in the receiving path precludes leakage from the receiving antenna which could be reflected by an unwanted close target, thereby causing false triggering.

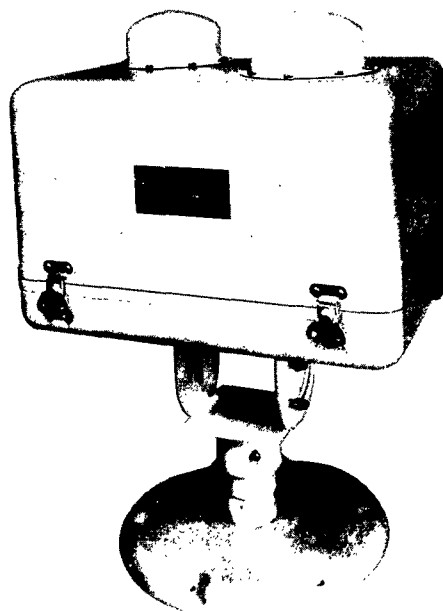
The cross-guide coupler directs a small amount of transmitter power to the crystal mixer as local-oscillator energy.

2. OSCILLATOR-MULTIPLIER SECTION

The oscillator-multiplier section consists of the oscillator that frequency-modulates the klystron and a multiplier circuit that multiplies the FM oscillator five times for use as the second mixer oscillator (Section II of Figure 1).



A. RUNWAY DETECTOR



B. APPROACH-ZONE DETECTOR

FIGURE 5. FM-CW X-BAND DETECTOR

FIGURE 6. SCHEMATIC DIAGRAM OF FM-CW DETECTOR

FIGURE 6 (SHEET 1 OF 2)

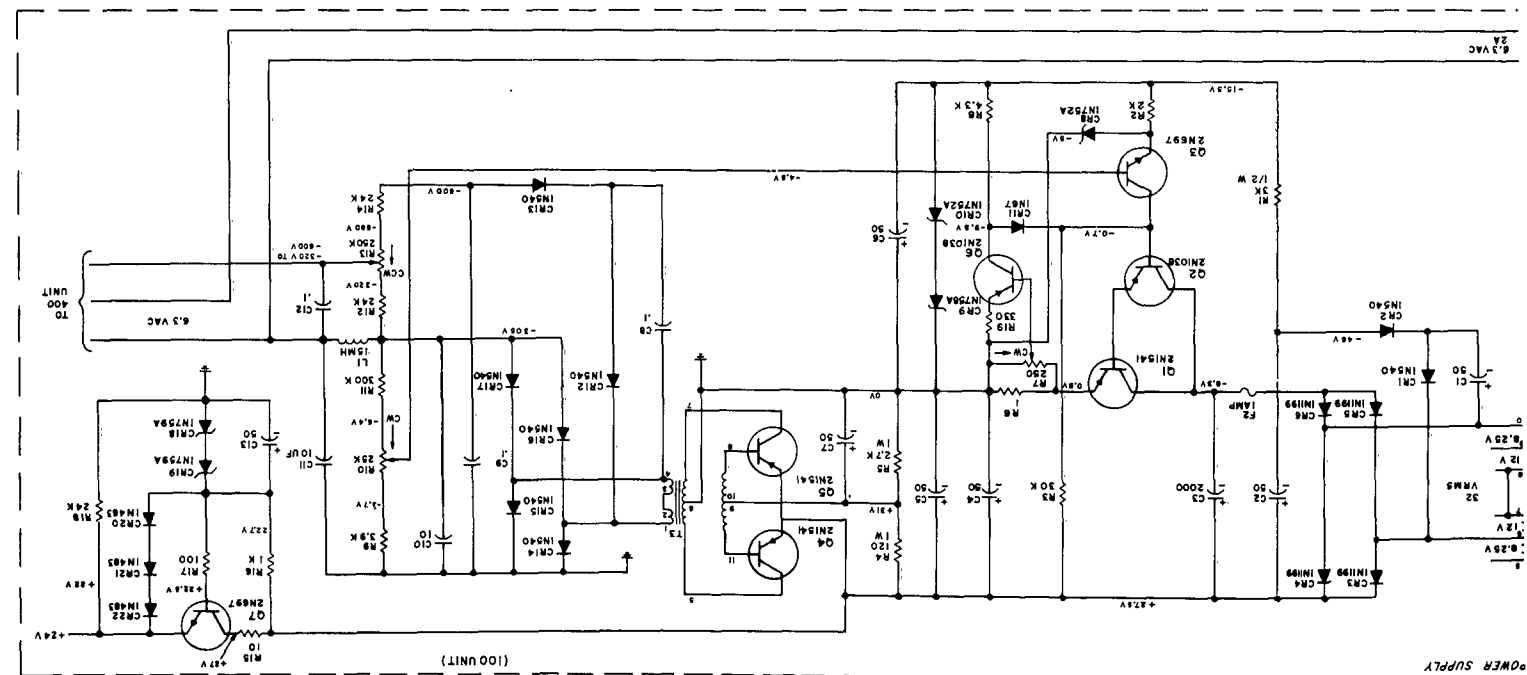
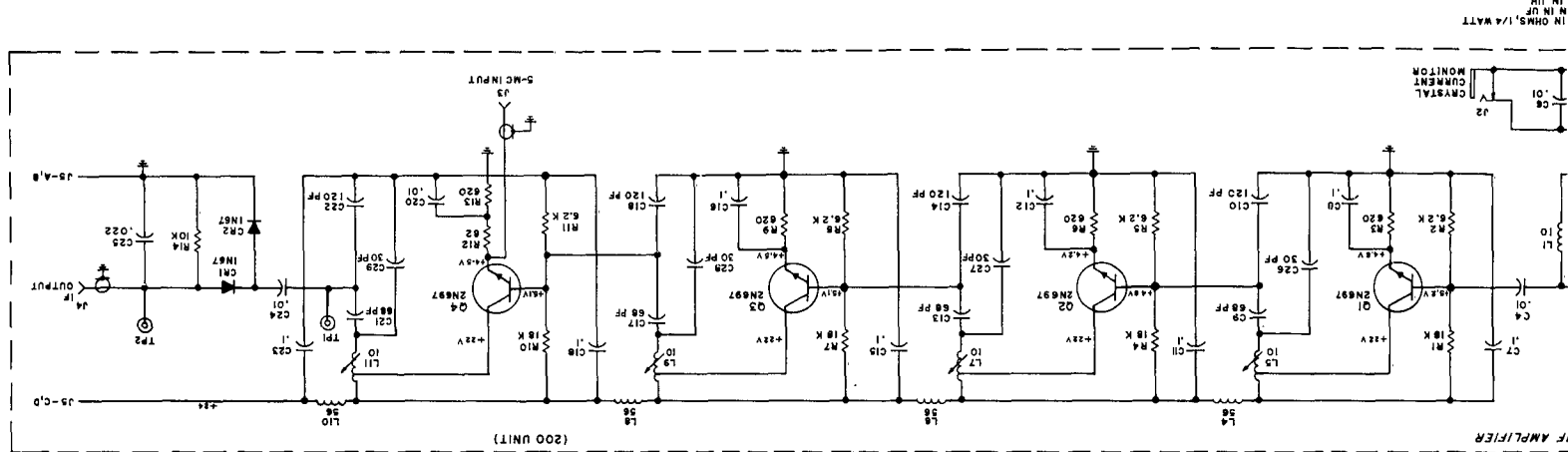
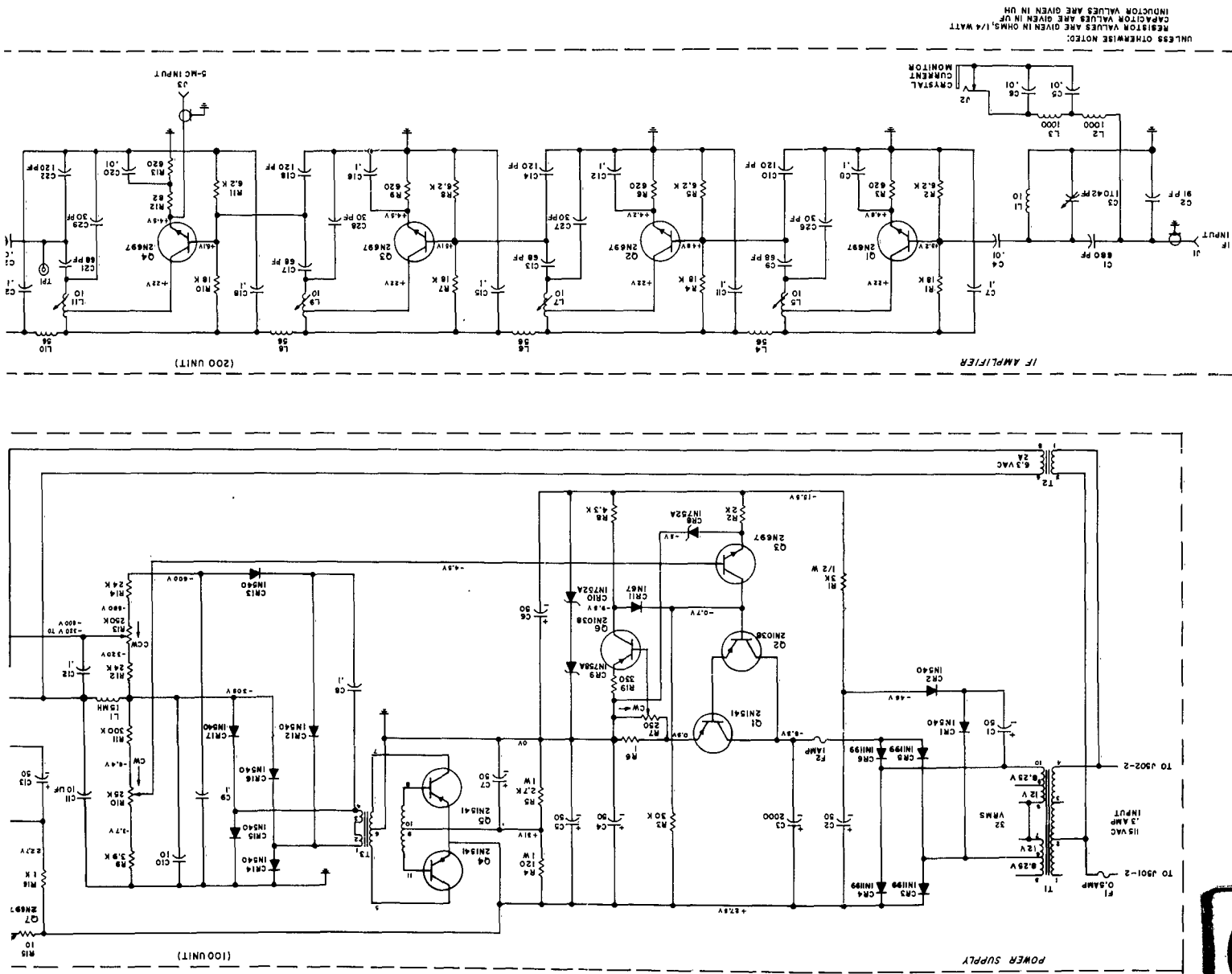
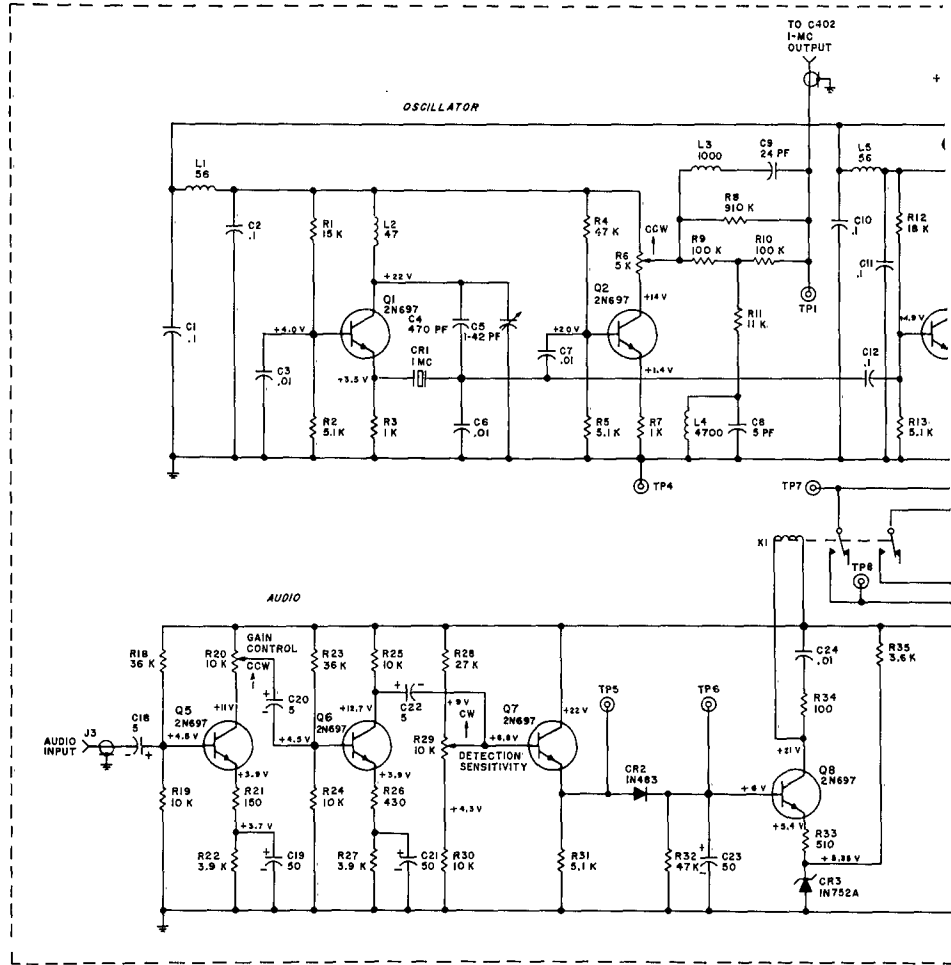


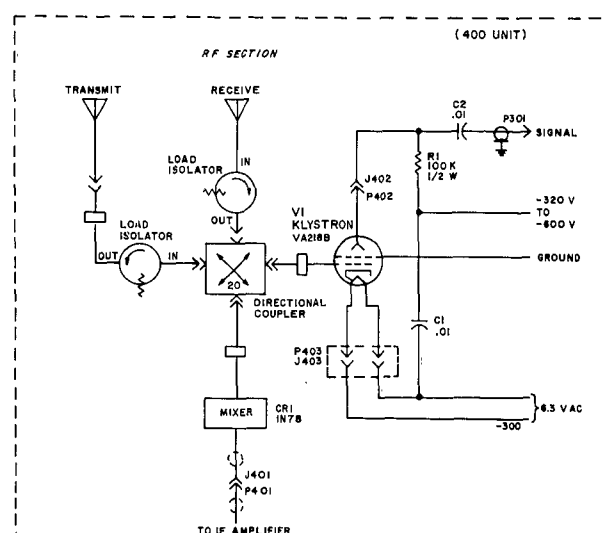
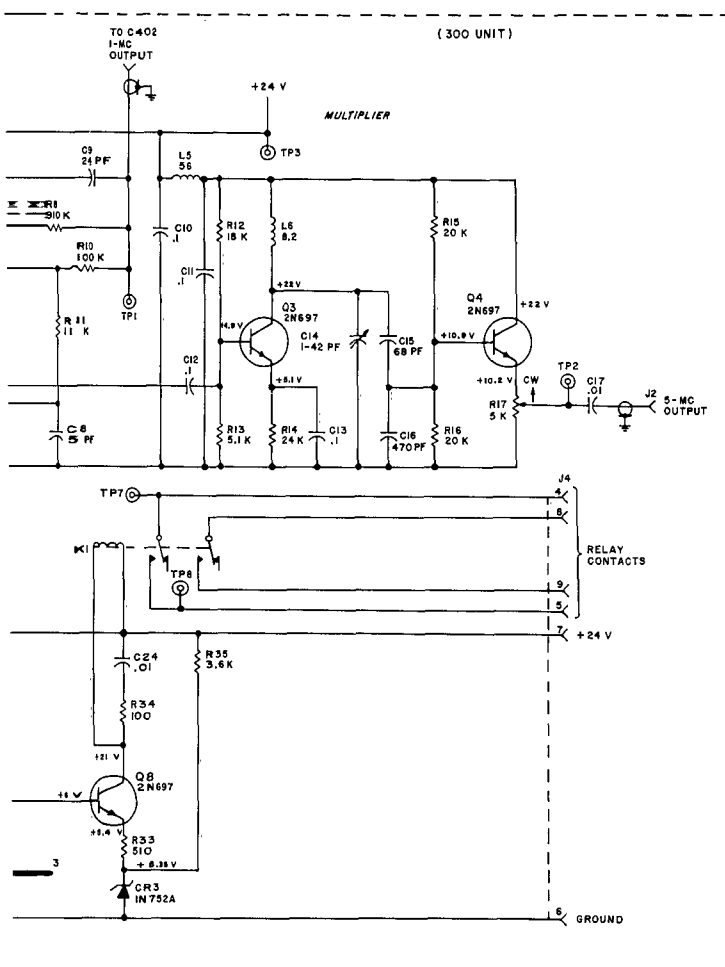
FIGURE 6. SCHEMATIC DIAGRAM OF FM-CW DETECTOR



2

1





UNLESS OTHERWISE NOTED:
RESISTOR VALUES ARE GIVEN IN OHMS, 1/4 WATT
CAPACITOR VALUES ARE GIVEN IN UF
INDUCTOR VALUES ARE GIVEN IN UH

FIGURE 6
(SHEET 2 OF 2)

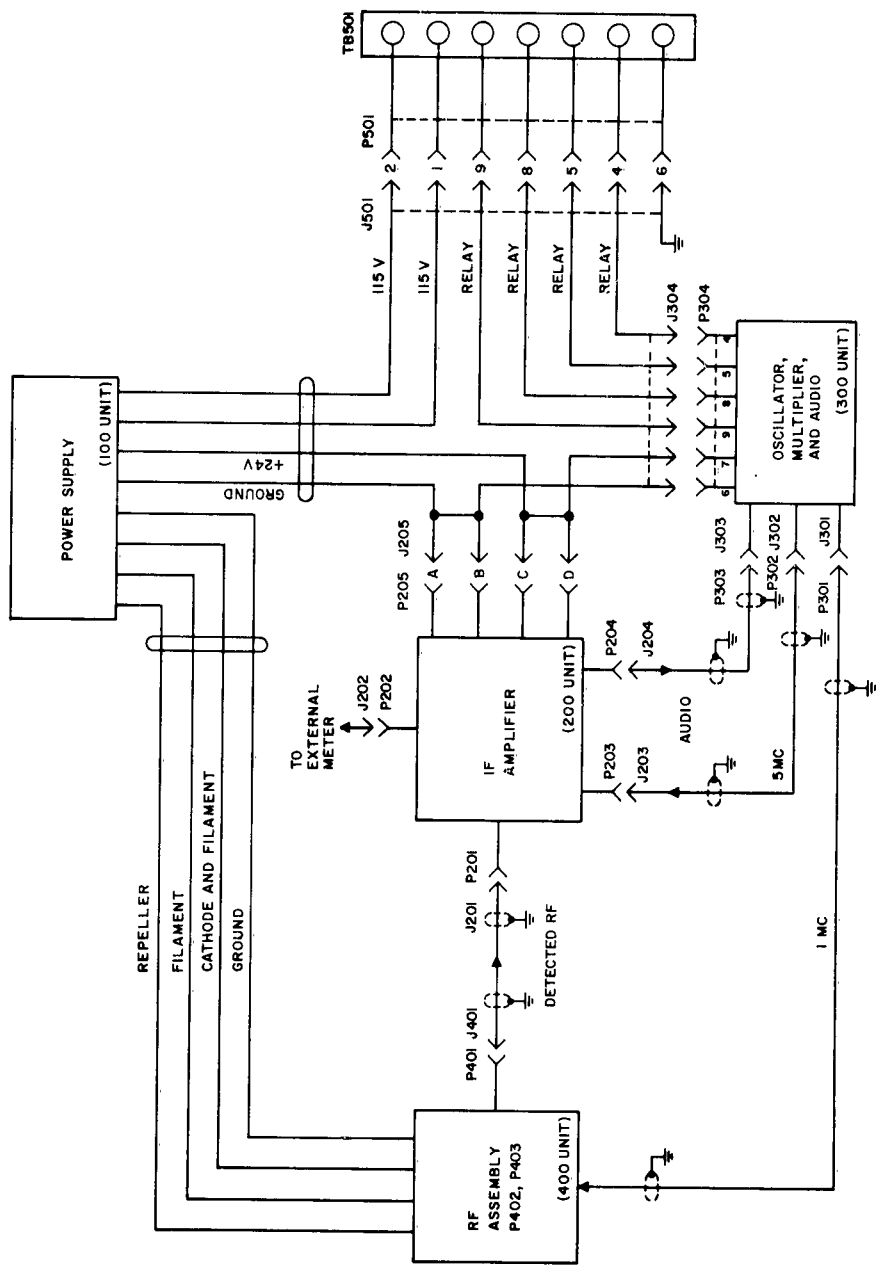


FIGURE 7. INTERCONNECTION DIAGRAM OF FM-CW DETECTOR

Figure 8 is a simplified schematic diagram of the oscillator-multiplier section. Q1 is a 2N697 silicon transistor in a crystal-controlled Colpitts oscillator circuit. This oscillator generates the modulation frequency to frequency-modulate the klystron. Q2 is a transistor amplifier that amplifies the oscillator frequency to the proper level for application to the klystron repeller.

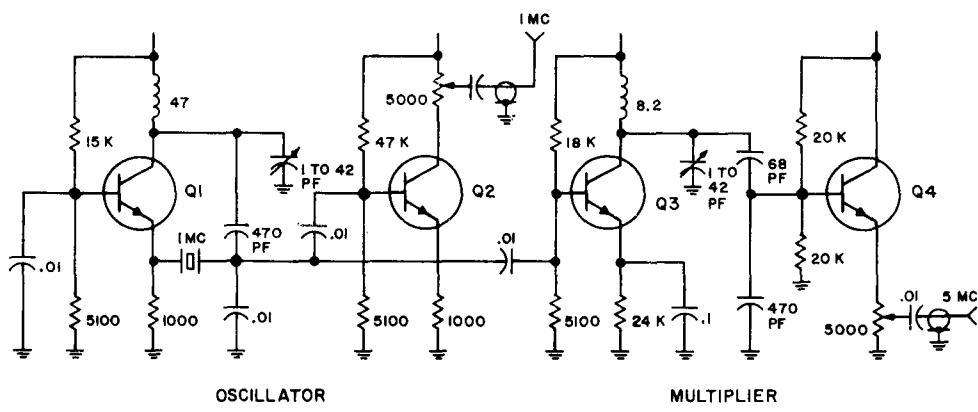
Transistor Q3 is used as a multiplier; its collector circuit is tuned to the fifth harmonic of the oscillator frequency. Q4 is an emitter-follower that isolates the multiplier circuit from the second mixer and delivers the fifth harmonic of the modulation frequency to the second mixer at a low impedance.

3. IF AMPLIFIER AND SECOND MIXER SECTION

Section III of Figure 1 is a block diagram of the IF amplifier and second mixer, and Figure 9 is a simplified schematic diagram of these components.

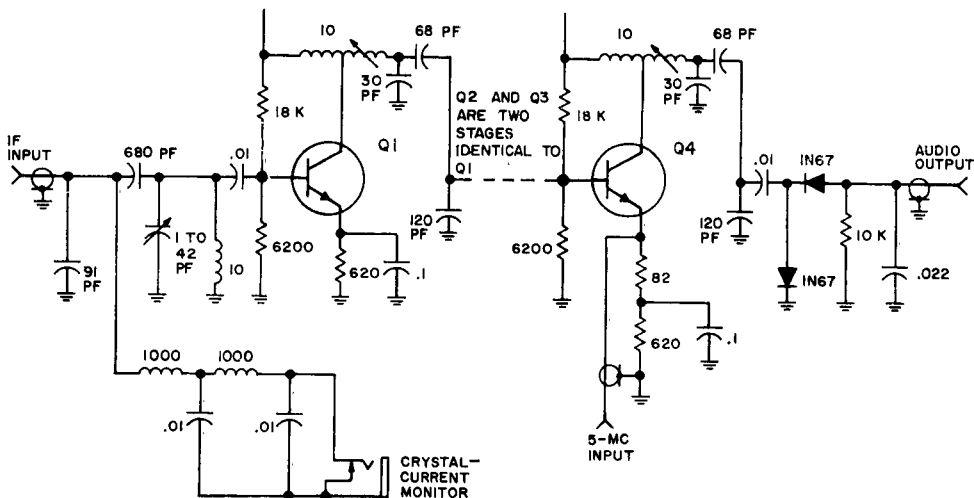
The output of the first mixer is applied to the IF input. The first mixer crystal current can be monitored on the IF chassis. The four-stage IF amplifier is tuned to the fifth harmonic of the modulation oscillator. Each stage is single tuned and uses an inductive tap to obtain a narrow bandwidth and a capacitive tap to match the impedance between stages.

The last stage of the IF amplifier (Q4) also acts as the second mixer. The multiplied modulation-oscillator frequency is applied to the emitter of Q4 across the un bypassed 82-ohm resistor, and the amplified IF signal is applied to the base of Q4. The difference frequency, due to the doppler shift produced by a moving target, appears as an amplitude-modulated signal at the collector of Q4. This modulation is detected by the voltage-doubler detector and is the audio output of the IF strip.



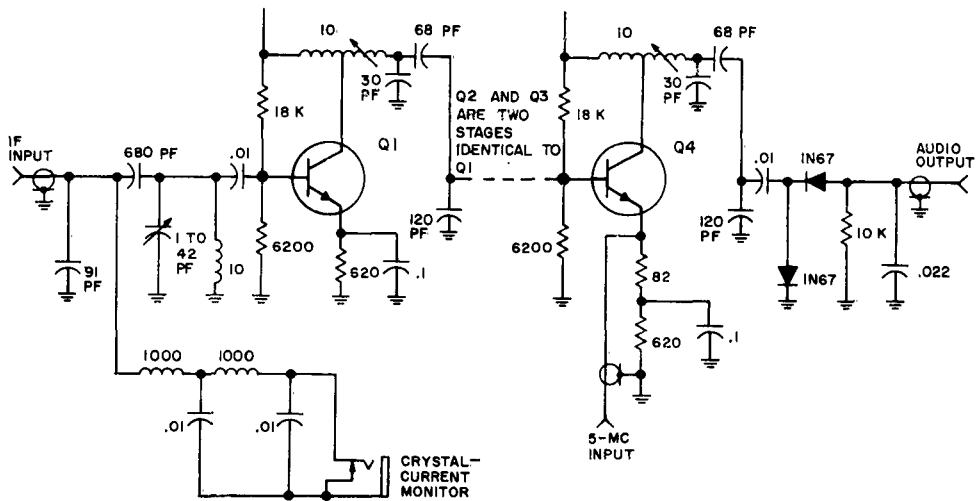
UNLESS OTHERWISE NOTED:
 RESISTOR VALUES ARE GIVEN IN OHMS
 CAPACITOR VALUES ARE GIVEN IN UF
 TRANSISTORS ARE TYPE 2N697

FIGURE 8. SIMPLIFIED SCHEMATIC DIAGRAM OF OSCILLATOR MULTIPLIER (300 UNIT)



UNLESS OTHERWISE NOTED:
 RESISTOR VALUES ARE GIVEN IN OHMS
 CAPACITOR VALUES ARE GIVEN IN UF
 TRANSISTORS ARE TYPE 2N697
 INDUCTOR VALUES ARE GIVEN IN UH

FIGURE 9. SIMPLIFIED SCHEMATIC DIAGRAM OF IF AMPLIFIER AND SECOND MIXER (200 UNIT)



UNLESS OTHERWISE NOTED:
 RESISTOR VALUES ARE GIVEN IN OHMS
 CAPACITOR VALUES ARE GIVEN IN UF
 TRANSISTORS ARE TYPE 2N697
 INDUCTOR VALUES ARE GIVEN IN UH

FIGURE 9. SIMPLIFIED SCHEMATIC DIAGRAM OF IF AMPLIFIER AND SECOND MIXER (200 UNIT)

4. AUDIO SECTION

Section IV of Figure 1 is the audio amplifier of the detector. Figure 10 is a simplified schematic diagram of the audio amplifier. Transistors Q5 and Q6 amplify the doppler signal. Transistor Q7 is an emitter-follower that drives the audio detector. Q8 is a normally nonconducting transistor with a relay in its collector circuit. Detected doppler signals place a positive voltage on the base of Q8, which conducts and energizes the relay indicating a moving target.

5. POWER SUPPLY SECTION

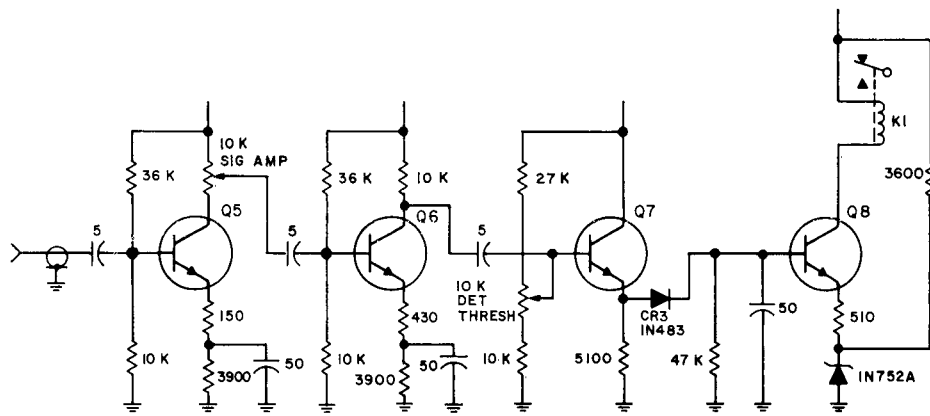
The power supply uses 115-volt 60-cps AC to produce voltages for the klystron and the transistor circuits (Figure 11).

A conventional transformer, bridge rectifier, and capacitor input filter supply about 34 volts DC to the regulator circuits. The high voltage for the klystron is obtained from a DC-to-DC converter circuit. The klystron voltages are regulated by obtaining an error signal at the high voltage, and using this signal to control the low-voltage DC applied to the DC-to-DC converter.

A filament transformer provides 6.3 volts AC at 2 amperes for the klystron filament.

A second series regulator, using the DC-to-DC converter primary voltage, supplies regulated voltage for the transistor circuitry of the detector.

Short-circuit protection is incorporated in the power supply to protect the power-supply transistors in case of short circuits.



UNLESS OTHERWISE NOTED:
 RESISTOR VALUES ARE GIVEN IN OHMS
 CAPACITOR VALUES ARE GIVEN IN UF
 TRANSISTORS ARE TYPE 2N697

FIGURE 10. SIMPLIFIED SCHEMATIC DIAGRAM OF AUDIO AMPLIFIER (300 UNIT)

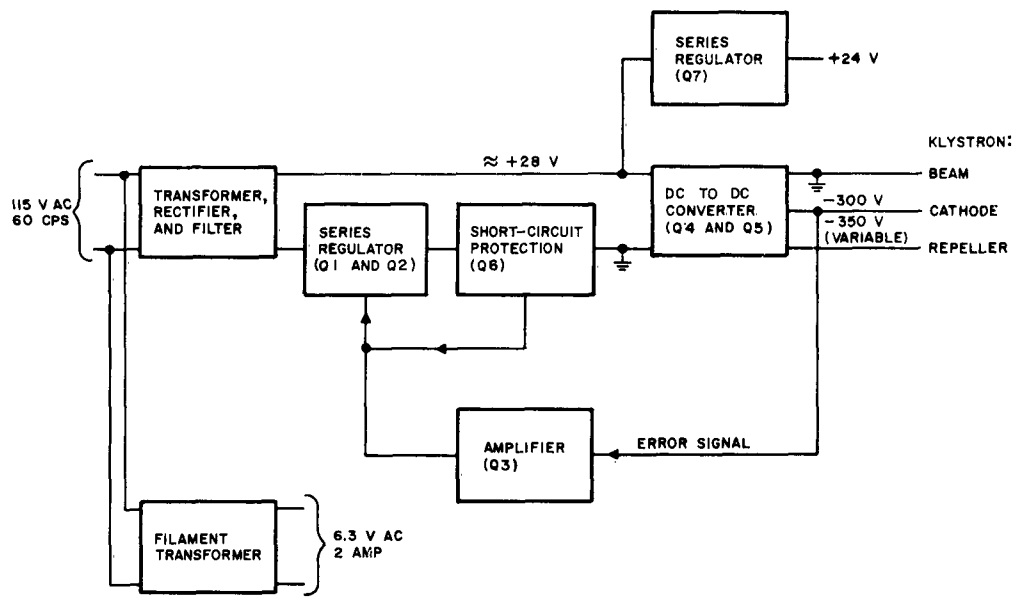


FIGURE 11. BLOCK DIAGRAM OF POWER SUPPLY (100 UNIT)

D. OPERATING PROCEDURES

1. INITIAL CONNECTION

The FM-CW detector is energized by applying 115 volts AC to terminals 1 and 2 of terminal board (TB) 501 in the bottom of the detector enclosure.

Detection of targets, indicated by relay contact closure, can be observed by attaching an ohmmeter to terminals 4 and 5 or 8 and 9 of TB501 or to test points (TP) 307 and 308. Actual signal return can be observed by connecting an oscilloscope to the audio output jack (TP306).

After applying power, an audible high-frequency tone will be heard by the operator. This is a normal phenomenon produced by the DC-to-DC converter that generates the operating voltages for the klystron.

As the klystron filaments warm up during the first 60 seconds of operation, the tube begins to draw current and the power-supply voltages stabilize near their normal operating points.

2. TEST PROCEDURE

If adjustments are to be made to the equipment, it is recommended that the unit be allowed to run for from 30 to 60 minutes before proceeding.

The first indication that the equipment is operating is the presence of crystal current, which indicates klystron oscillation. This current can be monitored by connecting a milliammeter to the miniature phone plug furnished with the equipment and inserting the plug at J202 on the IF chassis. Normal crystal current is 0.2 to 0.6 ma.

All DC voltage measurements can be made with a multimeter, except the klystron repeller voltage (variable between -320 and -600 volts), which must be made with a VTVM.

The klystron beam voltage is set at -300 volts by adjusting the beam adjust control (R110) on the power supply while monitoring the voltage adjustment at the klystron terminal board. Repeller voltage is set at about -355 volts by adjusting R113 while monitoring it with a VTVM at the klystron terminal board. The VTVM should not be left at this point because even its high input impedance will load the klystron. After removing the VTVM, R113 can be trimmed for maximum crystal current.

The over-current adjustment (R107) adjusts the level at which circuit protection transistor (Q106) begins to limit power-supply current. Because this adjustment can reduce even normal current, it should not be moved from the range where it does not affect beam voltage and converter frequency.

All the transistor circuits use 24-volt DC; this voltage can be monitored but cannot be adjusted. Its value is fixed by zener diodes CR118 and CR119 in the base circuit of Q107.

The 1-Mc modulating voltage for the klystron should be adjusted only when a spectrum analyzer is available to monitor the RF output spectrum. The analyzer need not be connected directly to the detector; sufficient energy can be coupled by connecting a length of coaxial cable to the analyzer and placing the open end of the cable near the transmitting antenna. Increased energy can be captured by using a waveguide-to-coaxial transition at the open end of the cable.

With the appropriate amount of 1-Mc modulating voltage applied to the klystron, an RF spectrum will result (Figure 12). If no 1 Mc is present, the spectrum will merge into the center frequency (f_0) and appear as one line of unmodulated carrier at 10.525 Gc. The sidebands occur at intervals of 1 Mc on each side of the center frequency. To achieve the symmetrical spectrum shown in Figure 12, it may be necessary to tune the klystron repeller below its maximum power setting. The klystron mode center for power does not necessarily correspond to the tuning mode center.

A fixed voltage (1 Mc) has not been specified because the modulation sensitivity of the klystron is subject to some variation from tube to tube. The amount usually required is about 3 volts when viewed with a probe whose input capacitance is .8 pf.

Adjustment of the 5-Mc amplitude (R306) and alignment of the synchronously tuned IF amplifier (200 unit), detection sensitivity (R329), and audio gain (R320) are best performed with a simulated signal.

To simulate the signal, an adjustable oscillator capable of operating around 5 Mc is needed. A Hewlett-Packard 650A or equivalent, with sufficient external attenuation to reduce the signal to -130 dbm, is recommended. This signal can be inserted at J201 in place of the normal detected RF and, by beating the signal with 5 Mc of the detector at the second mixer, an audio frequency output will be obtained.

The level of this signal, determined by the amount of attenuation which must be removed to cause relay operation, is an indication of detector sensitivity.

R320, the audio gain control, can be adjusted to give the desired signal amplitude for a given target. R329,

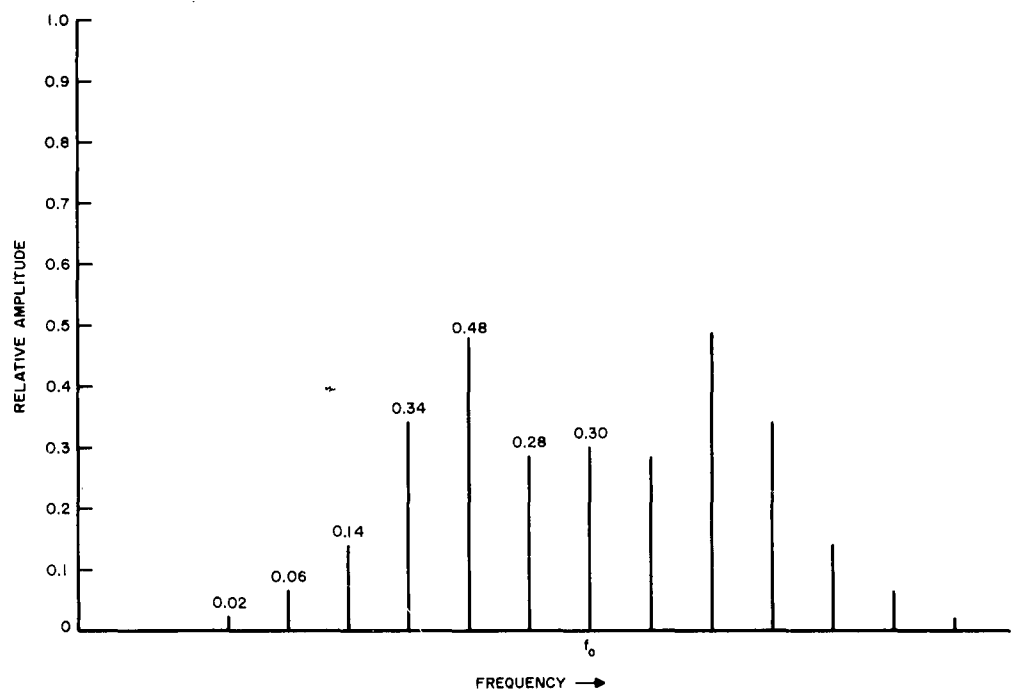


FIGURE 12. LINE SPECTRUM RESULTING FROM MODULATION INDEX OF 3.2

the sensitivity control, adjusts the operating threshold for the detection relay. R306, the 5-Mc amplitude adjustment, is adjusted to ensure that the maximum signal is obtained from the IF amplifier without oscillation in the audio circuitry.

With R320 set to maximum clockwise or highest gain, the unit is capable of detecting a simulated target whose level is below -120 dbm.

IV. DUAL-ANTENNA S-BAND DETECTORS

The modification of a single-antenna approach-zone detector and a single-antenna runway into a dual-antenna unit was performed by the Automatic Signal Division of Laboratory for Electronics. This modification eliminates the detection of rain and small objects close to the detector by having separate transmitting and receiving antenna patterns that do not intersect until they are several feet in front of the detector. Thus, an object must be several feet from the detector before it can cause detection. The modified runway detector is shown in Figure 13.

Figure 14 is a block diagram of the modified runway detector. The cavity of the 2C40 transmitting tube has been modified by adding a probe to extract RF energy for local-oscillator power. The 20-db pad isolates the transmitter source from the balanced mixer. An incoming signal mixes with the local-oscillator signal and produces a balanced signal (symmetrical with respect to ground) at the output of the mixer. Matched pairs of Type 1N21B crystals are used in the runway detector and Type 1N23E crystals in the approach-zone detector. Screw adjustments are provided on the mixer assembly to balance crystal mismatch and obtain the maximum reduction of local-oscillator signal to the receiving antenna. When matched pairs of crystals with high front-to-back ratios are used, the mixer adjustment is not critical.

The balanced mixer and the 20-db pad considerably reduce any variations in local-oscillator amplitude that could produce an output signal. A transformer is used to impedance-match between the mixer and vacuum tube amplifier and to convert the balanced signal to an unbalanced one.

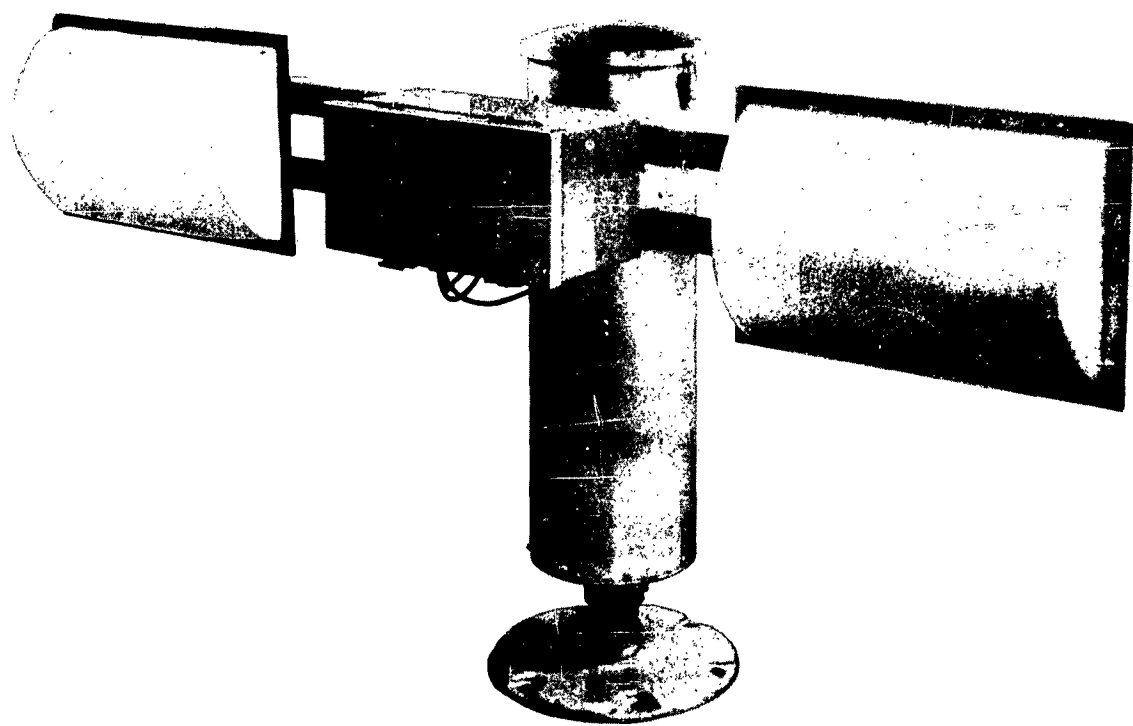


FIGURE 13. DUAL-ANTENNA S-BAND RUNWAY DETECTOR

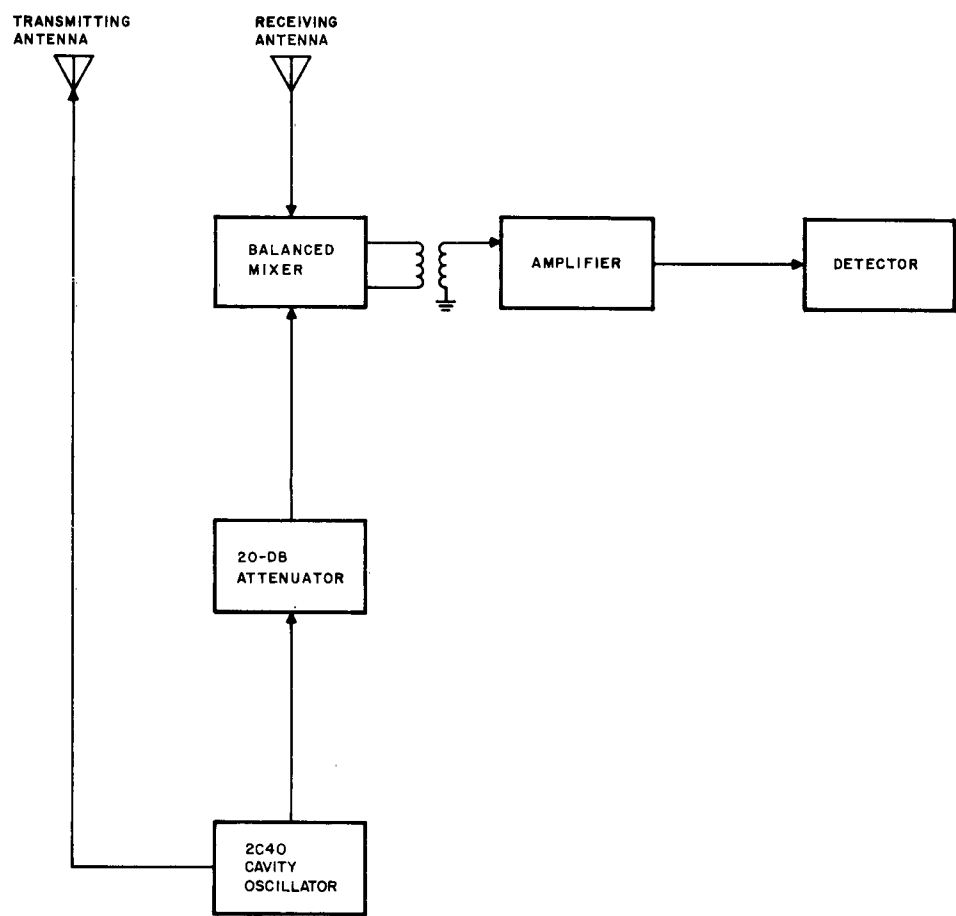
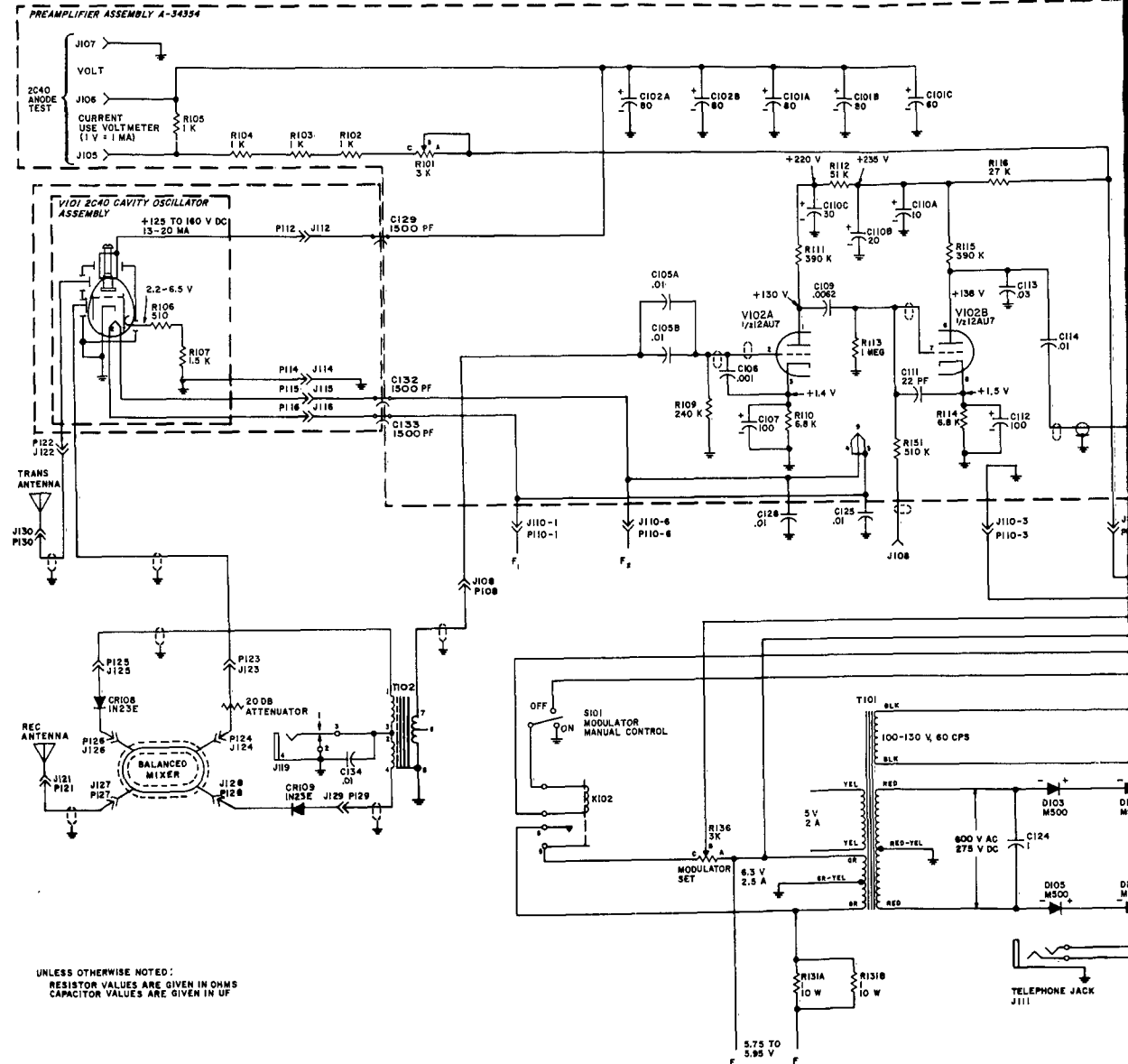


FIGURE 14. BLOCK DIAGRAM OF DUAL-ANTENNA S-BAND DETECTOR

The remainder of the detector is unmodified and, as previously reported in Report 5934-1, amplifies a doppler return, detects the presence of a doppler signal, and actuates a relay to indicate a target. Operating voltages are shown on the schematic diagram (Figure 15).



UNLESS OTHERWISE NOTED:
RESISTOR VALUES ARE GIVEN IN OHMS
CAPACITOR VALUES ARE GIVEN IN UF

11

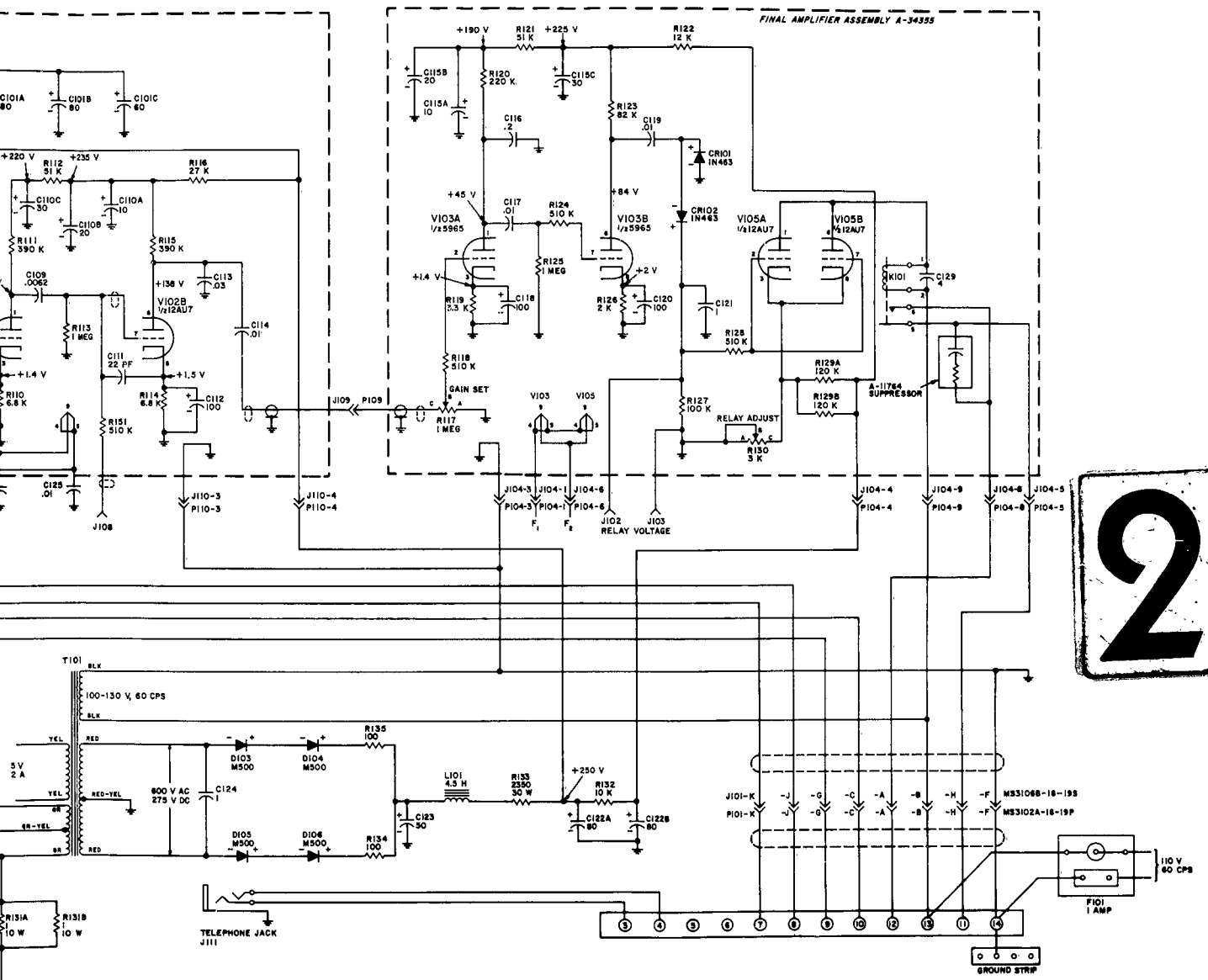


FIGURE 15. SCHEMATIC DIAGRAM OF APPROACH-ZONE DUAL-ANTENNA S-BAND DETECTOR

V. AUDIO ANALYSIS EQUIPMENT

The audio analysis equipment contains tape recording and signal-filtering facilities capable of processing returns from either the X-band or S-band doppler detectors (Figure 16).

Figure 17, a block diagram of the audio analysis equipment, shows the signal flow within the unit. Audio from the detector is inserted at the signal input and routed to the tape recorder and filter bank simultaneously. Voice commentary can be added to the recording by using a microphone furnished with the equipment. For processing pre-recorded data, the input is switched to PLAYBACK AND FILTER.

The filter bank is capable of dividing a signal within the detector pass band into six octave-wide components with center frequencies of 62.5, 125, 250, 500, 1000, and 2000 cps (Figure 17). These components can be used as filtered or further processed by detection to be used as DC voltages to drive, for example, a pen recorder (Figure 18).

It is expected that this equipment will prove to be a valuable tool in cataloging the characteristics of the various returns encountered during evaluation.

Propeller modulation, for example, is thought to cause a large portion of the return signal from light aircraft. Little is known, however, about its frequency components. By taxiing a light aircraft past a detector with a series of different engine rpm's but with a fixed ground speed, a correlation between propeller speed and frequency should be evident at the audio analysis equipment.

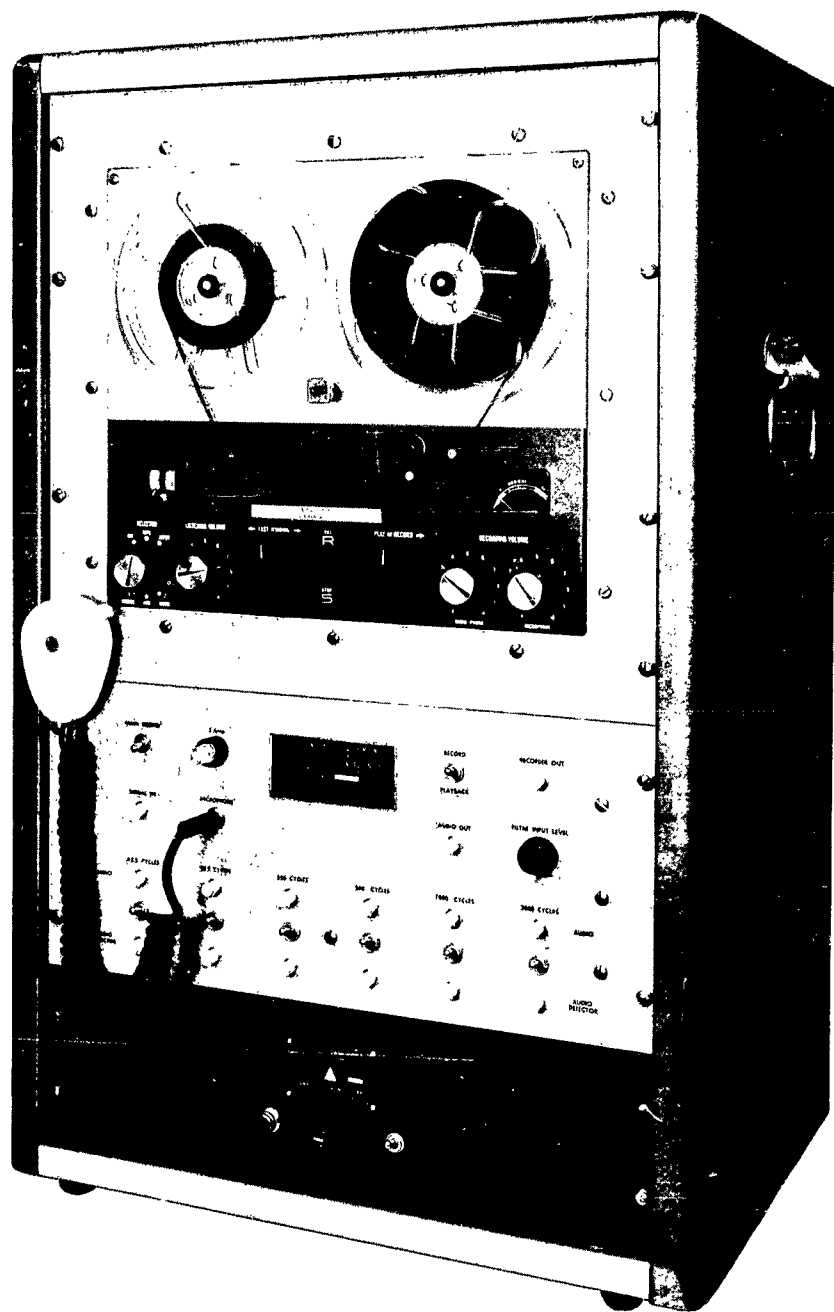


FIGURE 16. AUDIO ANALYSIS EQUIPMENT

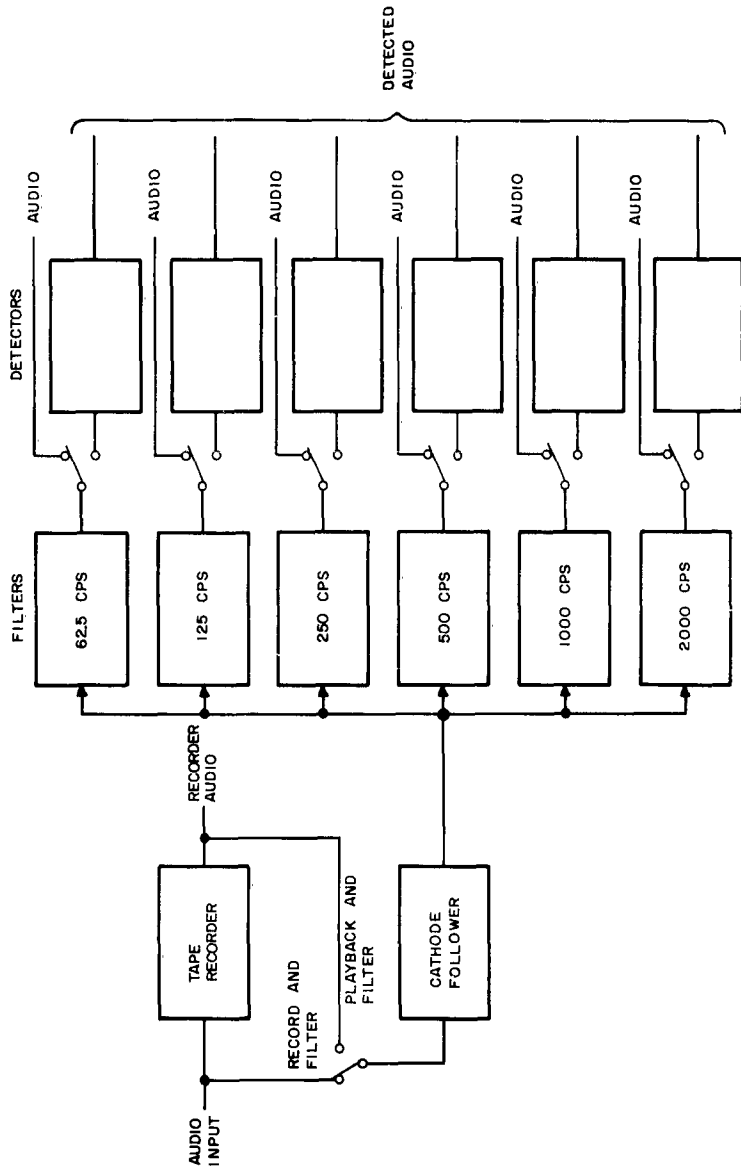
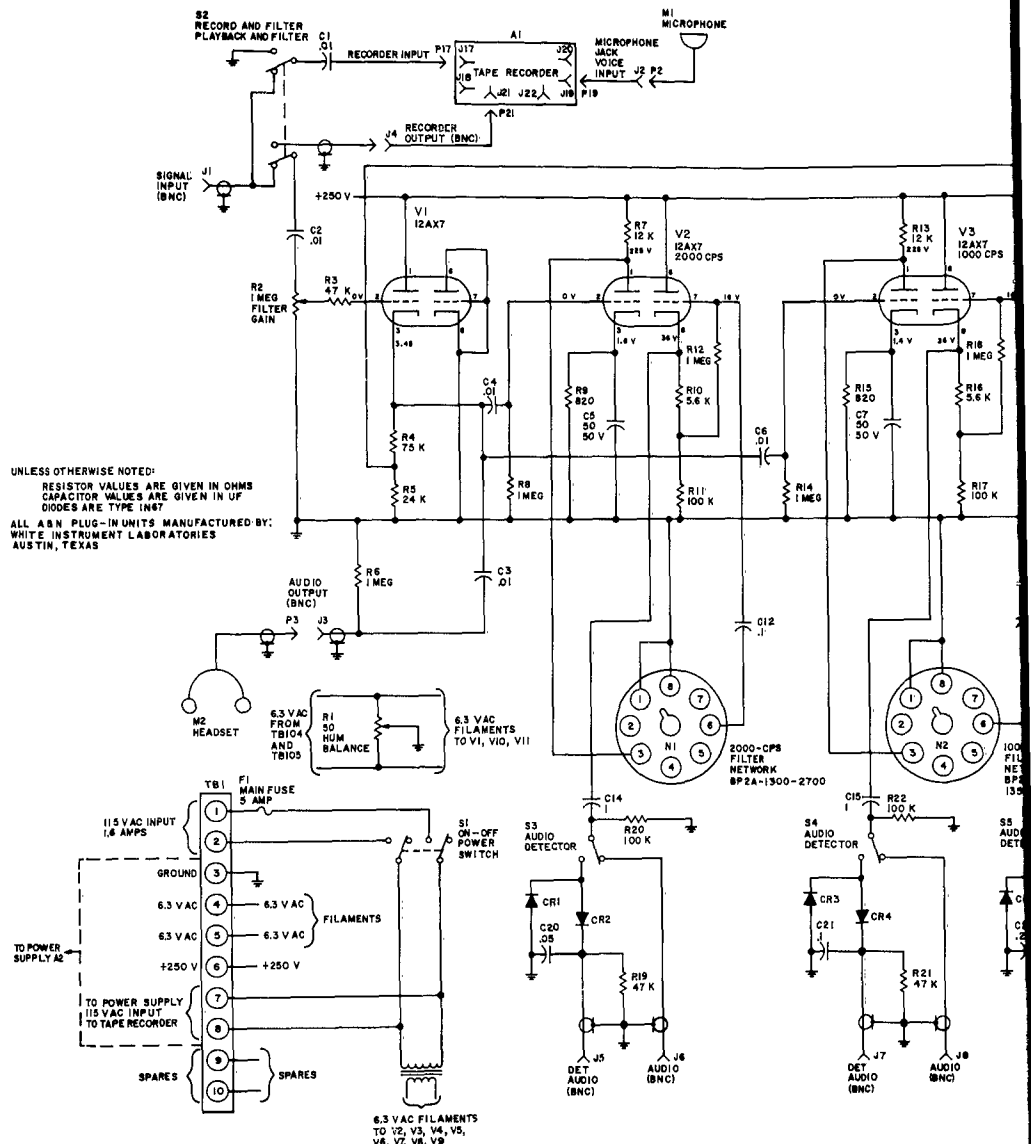


FIGURE 17. BLOCK DIAGRAM OF AUDIO ANALYSIS EQUIPMENT

1



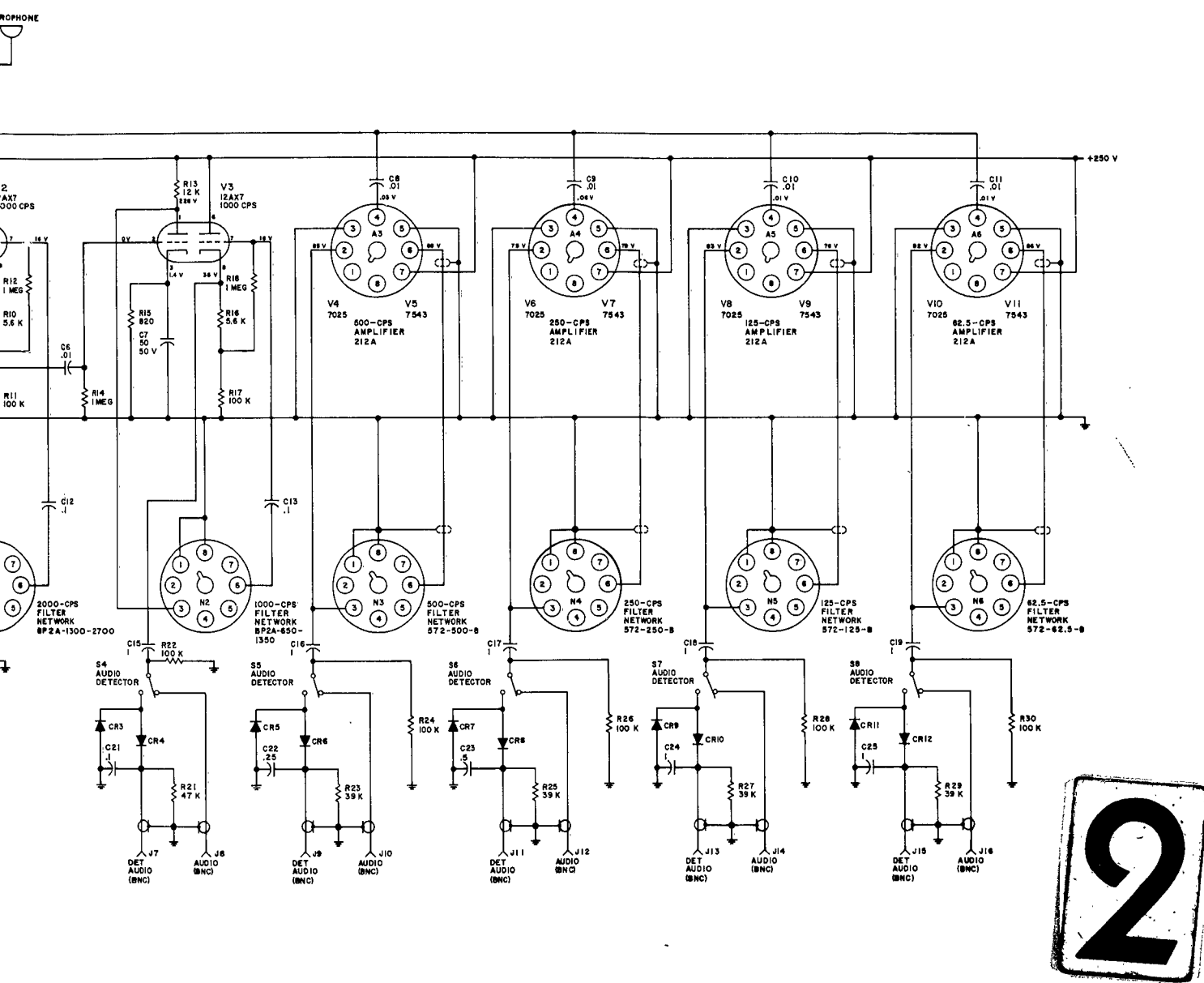


FIGURE 18. SCHEMATIC DIAGRAM OF AUDIO ANALYSIS EQUIPMENT

With passing target returns, the signal pattern is: high frequency, followed by low frequency, passing through zero, and returning to high frequency. Extraneous returns lack this characteristic pattern.

The analysis equipment can be used during evaluation as an input to a six-channel pen recorder to verify and further describe this target-frequency characteristic. Should sequential excitation of adjacent filter channels prove to be an absolutely reliable indicator of target validity, future equipment might incorporate recognition circuits to further enhance system performance.